Hindawi Publishing Corporation
EURASIP Journal on Wireless Communications and Networking
Volume 2009, Article ID 436756, 10 pages
doi:10.1155/2009/436756

Research Article

Estimation of CFO and Channels in Phase-Shift Orthogonal Pilot-Aided OFDM Systems with Transmitter Diversity

Carlos Ribeiro[1] and Atílio Gameiro[2]

[1] *Escola Superior de Tecnologia e Gestão, Instituto Politécnico de Leiria, Morro do Lena, Alto Vieiro, 2411-901 Leiria, Portugal*
[2] *Instituto de Telecomunicações, Universidade de Aveiro, 3810-193 Aveiro, Portugal*

Correspondence should be addressed to Carlos Ribeiro, cribeiro@estg.ipleiria.pt

Received 1 July 2008; Revised 4 November 2008; Accepted 23 January 2009

Recommended by Mounir Ghogho

We present a CFO estimation algorithm and an associated channel estimation method for broadband OFDM systems with transmitter diversity. The CFO estimation algorithm explores the TD structure of the transmitted symbols carrying pilots and data, relying solely on the data component present on the symbols to estimate the CFO, thus avoiding additional overhead like training symbols or null subcarriers. An intermediate output of the CFO algorithm provides an easy-to-get initial CIR estimate that will be improved with the utilization of a TD LMMSE filter. The feasibility of the investigated methods is substantiated by system simulation using indoor and outdoor broadband wireless channel models. Simulation results show that the joint algorithms provide a near optimal system's performance.

1. Introduction

Future mobile broadband applications will require reliable high data-rate wireless communication systems. In recent years, multiple-input multiple-output orthogonal frequency division multiplexing (MIMO-OFDM) transmission systems [1–4] emerged as the scheme with the potential to fulfill these conditions, with bandwidth efficiency and robustness to frequency selective channels, common in mobile personal communication systems.

Various forms of OFDM have been adopted in different standards: WIMAX, LTE, IEEE.802.11a/g [5], IEEE.802.16 [6], and DAB/DVB [1]. However, the long symbol duration makes OFDM systems particularly sensitive to carrier frequency offsets (CFOs) that always exist between the base station (BS) and mobile terminal (MT). The presence of CFO destroys the orthogonality among subcarriers leading to intercarrier interference (ICI), that causes severe degradation of the system's bit error rate (BER) [7–9].

The estimation and removal of the CFO has been the focus of a considerable number of works published in recent years. The algorithms can be categorized as blind or data-aided. The first category explores the properties of the received symbols (commonly the cyclic prefix (CP)) [10–12]. The data-aided algorithms use dedicated training symbols [13, 14] or exploit the presence of null subcarriers [15, 16].

The accurate extraction of the channel state information is crucial to realize the full potential of the MIMO-OFDM system. The performance of the channel estimator is vital for diversity combining, coherent detection and decoding, and resource allocation operations. The cochannel interference inherent to the system, where the received signal is the superposition of the signals transmitted simultaneous from the different antennas, puts an additional challenge on the design of the channel estimation algorithm.

A decision-directed channel estimation scheme that attempted to minimize the cochannel interference was published in [17]. The proposed algorithm exhibits a high computational load. A simplified and enhanced algorithm, introducing a data-aided scheme for the data transmission mode, is presented in [18]. The topic attracted a significant attention and has been the focus of investigation in multiple publications [19–21] and references therein.

The design of training symbols and pilot sequences with the ability to decouple the cochannel interference and minimize the channel estimation mean square error (MSE)

for MIMO-OFDM was addressed in several publications [18, 22, 23].

Most publications on the topic of training-signal or pilot-aided channel estimation use the frequency-domain (FD) *least squares* (LS) estimates as the starting point for the analysis of the estimation algorithm or the design of the training sequence. It was established in [24] that in single-input single-output (SISO) OFDM a time-domain (TD) equivalent to LS estimate could be obtained using a simple linear operation on the received signal, if the used pilot sequence fulfills certain conditions.

This paper contains a proposal for a CFO estimation algorithm and associated channel estimation method for OFDM systems with transmitter diversity that exploits a standardized transmission format, where FD pilot symbols are regularly spread in the OFDM symbols. To minimize the pilot overhead, the pilot subcarriers are shared among all transmit antennas. To mitigate the resulting cochannel interference, the system adopts phase-shifted pilot sequences per transmit antenna [18]. By exploring the TD properties of the received symbols, the proposed algorithms are able to estimate and remove the CFO, separate each of the CIRs, and generate the final channel estimate, without requiring any additional overhead (training symbols or null subcarriers). By performing most of the operations on the TD received symbols and sharing operations, the overall computational load required to implement both algorithms is affordable for real-time implementations.

The paper is organized as follows. Section 2 gives a brief introduction to the wireless multipath channel and the OFDM baseband model. In Section 3, the investigated CFO and channel estimation algorithms are developed. The feasibility of the developed method is substantiated by simulation results presented in Section 4. Finally, conclusions are drawn in Section 5.

2. OFDM in Mobile Wireless Channels

Before introducing the investigated method, we will briefly overview the mobile wireless multipath channel and the considered OFDM baseband model.

Throughout the text, the notation $(\sim)$ is used for TD vectors and elements, and its absence denotes frequency-domain (FD) vectors and elements. The index n denotes TD elements and k FD elements. Unless stated otherwise, the vectors involved in the transmission/reception process are column vectors with N_C complex elements. The superscripts $(\cdot)^T$ and $(\cdot)^H$ denote transpose and Hermitian transpose, respectively.

2.1. The Wireless Multipath Channel. Let us consider that the system transmits over multipath Rayleigh fading wireless channels modeled by the discrete-time channel impulse response (CIR):

$$\widetilde{h}[n] = \sum_{l=0}^{L_p-1} \alpha_l \delta[n-\tau_l], \tag{1}$$

where L_p is the number of channel paths, α_l and τ_l are the complex value and delay of path l, respectively. The paths are assumed to be statistically independent, with normalized average power, $\sum_{l=0}^{L_p-1} \sigma_h^2[l] = 1$, where $\sigma_h^2[l]$ is the average power of path l. The channel is time variant due to the motion of the mobile terminal (MT), but we will assume that the CIR is constant during one OFDM symbol. The time dependence of the CIR is not present in the notation for simplicity. Assuming that the insertion of a long enough cyclic prefix (CP) in the transmitter assures that the orthogonality of the subcarriers is maintained after transmission, the channel frequency response (CFR) can be expressed as

$$h[k] = \sum_{l=0}^{L_p-1} \alpha_l \exp\left(-j\frac{2\pi}{N_C}k\tau_l\right), \tag{2}$$

where N_C is the total number of subcarriers of the OFDM system.

2.2. OFDM Baseband Model. Consider the OFDM baseband system with n_S transmit antennas depicted in Figure 1. The n_S vectors $\mathbf{d}_s$ hold the M-ary PSK or QAM coded data to be transmitted.

To assist in the channel estimation process, pilot symbols are added in each transmit antenna path. The n_S vectors $\mathbf{p}_s$ hold the pilot values for each path. The pilots are transmitted in dedicated subcarries (vectors $\mathbf{p}_s$ and $\mathbf{d}_s$ contain nonzero values in disjoint positions). The resulting FD signal transmitted by antenna s is $\mathbf{s}_s = \mathbf{d}_s + \mathbf{p}_s$. All transmit antennas use the common set of subcarriers $\wp$ to convey the overlapping pilot sequences. The pilots are regularly spread every N_f subcarriers. The pilot separation can range from 1 (particular case where all subcarriers in the OFDM symbol are dedicated to transmit pilots–training symbol) to N_C, fulfilling the condition $N_C/N_f n_S \in \mathbb{N}$.

The system uses distinct phase-shifted pilot sequences in each transmit antenna to allow the separation of the sequences in the receiver. The kth element of the vector $\mathbf{p}_s$ is defined by

$$p_s[k] = \sum_{m=0}^{N_t-1} \delta[k - k_{\text{ini}} - mN_f] \exp\left(-j2\pi\frac{s}{n_S}m\right), \tag{3}$$

where $N_t = N_C/N_f$, and $k_{\text{ini}} \in \{0, \ldots, N_f - 1\}$ is the first pilot subcarrier.

The inverse discrete Fourier transform (DFT) block present in each antenna path transforms the input vector into the TD vector $\widetilde{\boldsymbol{s}}_s$, using an efficient N_C-points inverse fast Fourier transform (FFT) algorithm.

An L samples long guard interval, in the form of CP, is prefixed to vector $\widetilde{\boldsymbol{s}}_s$, resulting in the TD transmitted vector

$$\widetilde{\boldsymbol{x}}_s = \mathbf{A}_{\text{CP}}\mathbf{F}^H\mathbf{s}_s = \mathbf{A}_{\text{CP}}(\widetilde{\boldsymbol{d}}_s + \widetilde{\boldsymbol{p}}_s), \tag{4}$$

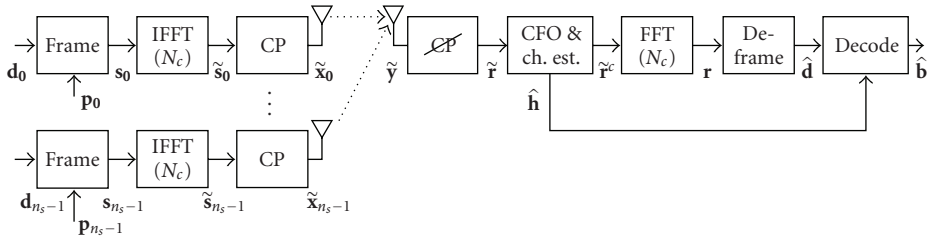

Figure 1: OFDM baseband system model.

where $\mathbf{F} \triangleq N_C^{-1/2} \exp(-j(2\pi/N_C)kn)_{k,n=0,0}^{N_C-1,N_C-1}$ is the $N_C \times N_C$ DFT matrix, and $\mathbf{A}_{\text{CP}} = [\mathbf{I}_{N_C,L} \ \ \mathbf{I}_{N_C}]^T$ is the matrix that adds the CP, with $\mathbf{I}_{N_C}$ denoting the $N_C \times N_C$ identity matrix and $\mathbf{I}_{N_C,L}$ denoting the last L columns of $\mathbf{I}_{N_C}$. The TD vectors $\tilde{\mathbf{d}}_s$ and $\tilde{\mathbf{p}}_s$ collect, respectively, the components of the data symbols and pilot symbols present in $\tilde{\mathbf{s}}_s$. The n_S vectors $\tilde{\mathbf{s}}_s$ are simultaneously transmitted to the receiver's antenna.

Let $w_o = 2\pi f_o \Delta t$ be the normalized angular CFO, where f_o is the frequency offset due to the frequency mismatch of the oscillators of the transmitter and the receiver, and Δt is the sampling interval.

The nth received signal sample of the ith symbol can be expressed as

$$\tilde{y}_i[n] = \exp\left[jw_o(i(N_C+L)+n)\right] \sum_{s=0}^{n_S-1} \sum_{l=0}^{L_p-1} \tilde{h}_{s,i}[l]\tilde{x}_{s,i}[n-l] + \tilde{\bar{n}}_i[n], \tag{5}$$

where $\tilde{\bar{n}}_i[n]$ is a sample of independent and identically distributed (*iid*) zero mean additive white Gaussian noise (AWGN) with variance σ_n^2. Collecting the $(N_C + L)$ samples of the symbol,

$$\tilde{\mathbf{y}}_i = \exp\left[jw_o i(N_C+L)\right] \mathbf{C}_{(N_C+L)}(w_o) \sum_{s=0}^{n_S-1} \tilde{\mathbf{H}}_{s,i}^{\text{lin}} \tilde{\mathbf{x}}_{s,i} + \tilde{\mathbf{z}}_i + \tilde{\bar{\mathbf{n}}}_i, \tag{6}$$

where the vector $\tilde{\bar{\mathbf{n}}}_i$ collects the noise samples that affect the ith symbol, the vector $\tilde{\mathbf{z}}_i$ represents the intersymbol interference (ISI) caused by the channel dispersion, and the matrix $\tilde{\mathbf{H}}_{s,i}^{\text{lin}}$ is the $(N_C+L)\times(N_C+L)$ lower triangular Toeplitz channel convolution matrix with first column $\tilde{\mathbf{h}}_{s,i}$ (column (N_C+L)-vector with the discrete-time CIR (its elements are defined by (1)) padded with zeros). The $(N_C+L)\times(N_C+L)$ diagonal matrix that holds the phase rotation that affects each symbol sample is

$$\mathbf{C}_{(N_C+L)}(w_o) = \text{diag}([1 \ \ \exp(jw_o) \ \ \cdots \ \ \exp\left[jw_o(N_C+L-1)\right]]). \tag{7}$$

The receiver starts by removing the CP from the received symbol. Dropping the symbol index, the resulting vector is

$$\begin{aligned}\tilde{\mathbf{r}} &= \mathbf{R}_{\text{CP}}\tilde{\mathbf{y}} \\ &= \exp\left[jw_o i(N_C+L)\right]\mathbf{R}_{\text{CP}}\mathbf{C}_{(N_C+L)}(w_o) \\ &\quad \times \sum_{s=0}^{n_S-1} \tilde{\mathbf{H}}_s^{\text{lin}}\tilde{\mathbf{x}}_s + \mathbf{R}_{\text{CP}}\tilde{\mathbf{z}} + \tilde{\mathbf{n}} \\ &= \theta_{\text{ini}}\mathbf{C}_{N_C}(w_o) \sum_{s=0}^{n_S-1} \mathbf{R}_{\text{CP}}\tilde{\mathbf{H}}_s^{\text{lin}}\mathbf{A}_{\text{CP}}\tilde{\mathbf{s}}_s + \mathbf{R}_{\text{CP}}\tilde{\mathbf{z}} + \tilde{\mathbf{n}},\end{aligned} \tag{8}$$

where $\mathbf{R}_{\text{CP}} = [\mathbf{0}_{(N_C\times L)} \ \ \mathbf{I}_{N_C}]$ is the matrix that removes the CP with $\mathbf{0}_{(N_C\times L)}$ representing the $(N_C \times L)$ null matrix, $\tilde{\mathbf{n}} = \mathbf{R}_{\text{CP}}\tilde{\bar{\mathbf{n}}}$ is the resulting TD noise column N_C-vector, and $\theta_{\text{ini}} = \exp[jw_o(i(N_C+L)+L)]$ is the common phase that affects all samples of the ith symbol. The last step in (8) was possible considering the structure of the matrices involved

$$\mathbf{R}_{\text{CP}}\mathbf{C}_{(N_C+L)}(w_o) = \exp(jw_oL)\mathbf{C}_{N_C}(w_o)\mathbf{R}_{\text{CP}}. \tag{9}$$

With the assumption that the length of the CP is larger than the duration of CIR, the ISI is completely removed, and (8) can be written as

$$\begin{aligned}\tilde{\mathbf{r}} &= \theta_{\text{ini}}\mathbf{C}_{N_C}(w_o) \sum_{s=0}^{n_S-1} \tilde{\mathbf{H}}_s^{\text{circ}}\tilde{\mathbf{s}}_s + \tilde{\mathbf{n}} \\ &= \theta_{\text{ini}}\mathbf{C}_{N_C}(w_o) \sum_{s=0}^{n_S-1} \mathbf{F}^H\mathbf{H}_s\mathbf{s}_s + \tilde{\mathbf{n}},\end{aligned} \tag{10}$$

where $\tilde{\mathbf{H}}_s^{\text{circ}} = \mathbf{R}_{\text{CP}}\tilde{\mathbf{H}}_s^{\text{lin}}\mathbf{A}_{\text{CP}}$ is the $N_C \times N_C$ circulant matrix with circulant vector $\tilde{\mathbf{h}}_s$ and, due to the properties of the DFT, $\mathbf{H}_s = \mathbf{F}\tilde{\mathbf{H}}_s^{\text{circ}}\mathbf{F}^H = \text{diag}(\mathbf{h}_s)$, with the elements of $\mathbf{h}_s$ defined by (2).

The CFO and channel estimation block is responsible for estimating both the CFO that affects the received samples and the n_S channels that disturbed the transmission process. Both estimation algorithms will be introduced in the next section. Moreover, this block is also responsible for reducing the CFO, using the estimated CFO value $\hat{w}_o$. This operation can be described by

$$\tilde{\mathbf{r}}_c = \theta_{\text{ini}}\mathbf{C}_{N_C}^H(\hat{w}_o)\mathbf{C}_{N_C}(w_o) \sum_{s=0}^{n_S-1} \mathbf{F}^H\mathbf{H}_s\mathbf{s}_s + \mathbf{C}_{N_C}^H(\hat{w}_o)\tilde{\mathbf{n}}. \tag{11}$$

It is clear that if $\hat{w}_o = w_o$, then $\mathbf{C}_{N_C}^H(\hat{w}_o)\mathbf{C}_{N_C}(w_o) = \mathbf{I}_{N_C}$, and the CFO is completely removed. As it will be demonstrated

in the next section, the CFO ambiguity remaining after this block is an integer multiple of the pilot subcarrier separation $N_f\Delta f$, where Δf is the subcarrier separation. This acquisition range should be sufficient for current OFDM systems; however coarse CFO estimation techniques [25] can be used to tackle this limitation, if proven necessary.

The DFT block transforms the vector $\widetilde{\mathbf{r}}$ to FD with an efficient FFT operation. Assuming that the CFO is completely eliminated, the resulting FD column N_C-vector can be expressed as

$$\mathbf{r} = \mathbf{F}\widetilde{\mathbf{r}}c = \theta_{\text{ini}} \sum_{s=0}^{n_S-1} \mathbf{H}_s\mathbf{s}_s + \mathbf{n}, \tag{12}$$

where $\mathbf{n} = \mathbf{F}\mathbf{C}_{N_C}^H(\widehat{w}_o)\widetilde{\mathbf{n}}$ is the resulting FD noise vector. The remaining phase-rotation θ_{ini} is naturally removed in the channel estimation process, assuming that the pilot-aided scheme calculates the LS estimates (back-rotated received signal).

The deframing block separates the signals in the subcarriers conveying pilots and data symbols. The values in the data subcarriers are collected in vector $\widehat{\mathbf{d}}$ and fed to the decoding block. Together with the channels' estimate $\widehat{\mathbf{h}}_s$, this block is now able to decode the received symbols, according to some decision rule, and generate the estimate of the transmitted data $\widehat{\mathbf{b}}$.

3. CFO and Channel Estimations by Exploring the TD Properties of Phase-Shifted Pilot Sequences

The algorithms implemented in this block estimate both the n_S channels over which the transmission occurred and the CFO that affects the received signal. The inputs to the CFO estimation algorithm are the TD symbols carrying both pilots and data, according to the model defined in the previous section. The channel estimation algorithm reuses an intermediate output of the previous operation to attain an initial CIR estimate with minimal computational load.

3.1. Analysis of the TD Symbol's Structure. From (10), each element of the TD received symbols (carrying pilots and data), after CP extraction, can be expressed by

$$\begin{aligned}&\widetilde{r}[n]\\ &= \theta_{\text{ini}} \exp(jw_o n) \sum_{s=0}^{n_S-1} \sum_{l=0}^{L-1} \widetilde{h}_s[l](\widetilde{d}_s[n-l] + \widetilde{p}_s[n-l]) + \widetilde{n}[n],\end{aligned} \tag{13}$$

where the elements of the TD data vector $\widetilde{\mathbf{d}}_s$ are

$$\widetilde{d}_s[n] = N_C^{-1/2} \sum_{\substack{k=0\\k\notin\wp}}^{N_C-1} d_s[k] \exp\left(j\frac{2\pi}{N_C}kn\right), \tag{14}$$

where $d_s[k]$ is the kth element of $\mathbf{d}_s$ (complex data symbol conveyed by the kth subcarrier of the s transmit antenna path), and the elements of the TD pilot vector $\widetilde{\mathbf{p}}_s$ are

$$\begin{aligned}\widetilde{p}_s[n] &= N_C^{-1/2} \sum_{k=0}^{N_C-1} \sum_{m=0}^{N_t-1} \delta[k - k_{\text{ini}} - mN_f]\\ &\qquad \times \exp\left(-j2\pi\frac{s}{n_S}m\right) \exp\left(j\frac{2\pi}{Nc}kn\right)\\ &= N_C^{1/2}N_f^{-1} \exp\left(j\frac{2\pi}{Nc}k_{\text{ini}}n\right) \sum_{m=0}^{N_f-1} \delta\left[n - \frac{s}{n_S}N_t - mN_t\right].\end{aligned} \tag{15}$$

Replacing (14) and (15) in (13),

$$\begin{aligned}\widetilde{r}[n] &= \theta_{\text{ini}}N_C^{-1/2} \exp(jw_o n)\\ &\quad \times \sum_{s=0}^{n_S-1} \sum_{l=0}^{L-1} \sum_{\substack{k=0\\k\notin\wp}}^{N_C-1} \widetilde{h}_s[l]d_s[k] \exp\left[j\frac{2\pi}{N_C}k(n-l)\right]\\ &\quad + \widetilde{n}[n] + \theta_{\text{ini}}N_C^{1/2}N_f^{-1} \exp(jw_o n)\\ &\quad \times \sum_{s=0}^{n_S-1} \sum_{l=0}^{L-1} \sum_{m=0}^{N_f-1} \widetilde{h}_s[l] \exp\left[j\frac{2\pi}{Nc}k_{\text{ini}}(n-l)\right]\\ &\qquad \times \delta\left[n - l - \frac{s}{n_S}N_t - mN_t\right]\\ &= \widetilde{r}^d[n] + \widetilde{r}^p p[n] + \widetilde{n}[n],\end{aligned} \tag{16}$$

where $\widetilde{\mathbf{r}}^d$ and $\widetilde{\mathbf{r}}^p$ hold the data-dependent and pilot-dependent components in $\widetilde{\mathbf{r}}$, respectively.

By expanding the pilot-dependent vector $\widetilde{\mathbf{r}}^p$

$$\begin{aligned}\widetilde{r}^p[n] &= \theta_{\text{ini}}N_C^{1/2}N_f^{-1} \exp(jw_o n)\\ &\quad \times \sum_{s=0}^{n_S-1} \sum_{m=0}^{N_f-1} \exp\left[j\frac{2\pi}{Nc}k_{\text{ini}}\left(mN_t + \frac{s}{n_S}N_t\right)\right]\\ &\qquad \times \widetilde{h}_s\left[n - \frac{s}{n_S}N_t - mN_t\right]\\ &= \theta_{\text{ini}}N_C^{1/2}N_f^{-1} \exp(jw_o n)\\ &\quad \times \sum_{m=0}^{N_f-1} \exp\left(j\frac{2\pi}{Nc}k_{\text{ini}}mN_t\right)\widetilde{h}_0[n - mN_t] + \cdots\\ &\quad + \theta_{\text{ini}}N_C^{1/2}N_f^{-1} \exp(jw_o n)\\ &\quad \times \sum_{m=0}^{N_f-1} \exp\left[j\frac{2\pi}{Nc}k_{\text{ini}}\left(mN_t + \frac{n_S-1}{n_S}N_t\right)\right]\\ &\qquad \times \widetilde{h}_{(n_S-1)}\left[n - \frac{n_S-1}{n_S}N_t - mN_t\right],\end{aligned} \tag{17}$$

it becomes clear that it is made up of N_f frequency-shifted and scaled replicas of each of the n_S CIR. Moreover, the replicas of each CIR are separated by N_t samples and transmit

antenna s CIR replicas are time-shifted $(s/n_S)N_t$ samples from the reference position mN_t, $m \in \{0, \ldots, N_f - 1\}$.

3.2. CFO Estimation. The CFO estimation method introduced in the following uses the pilot structures, introduced primarily for channel estimation purposes, to estimate the CFO present in the received samples. Therefore, it is absolutely bandwidth efficient, as it does not require any additional specific overhead. The algorithm exhibits a fast acquisition, being able to output an estimate with low deviation from a single OFDM frame. It proves adequate for burst mode transmission, where the frequency offset varies from frame to frame.

The algorithm requires a search within the acquisition range to find the minimum value of the cost function. An initial candidate angular frequency offset $\hat{w}$ is applied to the input signal $\tilde{\mathbf{r}}_i$, together with the TD equivalent of the FD multiband filter that selects the pilot subcarriers [24] (phase-shifted sum of the samples in the same relative position in all N_f segments of N_t samples). This operation can be described by

$$\tilde{\mathbf{g}} = \mathbf{T}\mathrm{diag}\left(\left[1 \;\; \exp\left(-j\frac{2\pi}{N_C}k_{\mathrm{ini}}\right) \cdots \exp\left[-j\frac{2\pi}{N_C}k_{\mathrm{ini}}(N_C-1)\right]\right]\right) \times \mathbf{C}_{N_C}^{H}(\hat{w})\tilde{\mathbf{r}} = \tilde{\mathbf{g}}d + \tilde{\mathbf{g}}p + \tilde{\mathbf{v}}, \tag{18}$$

where the $(N_t \times N_C)$ matrix $\mathbf{T} = [\mathbf{I}_{N_t} \cdots \mathbf{I}_{N_t}]$, the column N_t-vectors $\tilde{\mathbf{g}}^d$ and $\tilde{\mathbf{g}}^p$ hold the data-dependent and pilot-dependent components in $\tilde{\mathbf{g}}$, respectively, and $\tilde{\mathbf{v}}$ is the resulting noise vector. The elements of $\tilde{\mathbf{g}}^p$ can be expressed by

$$\begin{aligned}\tilde{g}^p[n] &= \sum_{m=0}^{N_f-1} \exp\left(-j2\pi k_{\mathrm{ini}}\frac{n+mN_t}{N_C}\right) \times \exp\left[-j\hat{w}(n+mN_t)\right]\tilde{r}^p[n+mN_t] \\ &= \theta_{\mathrm{ini}}N_C^{1/2}N_f^{-1}\exp\left[j(w_o-\hat{w})n\right] \times \sum_{s=0}^{n_S-1}\sum_{m=0}^{N_f-1}\sum_{q=0}^{N_f-1} \exp\left[-j\frac{2\pi}{Nc}k_{\mathrm{ini}} \times \left(n+(m-q)N_t - \frac{s}{n_S}N_t\right)\right] \\ &\quad \times \exp\left[j(w_o-\hat{w})mN_t\right]\tilde{h}_s\left[n-\frac{s}{n_S}N_t+(m-q)N_t\right].\end{aligned} \tag{19}$$

If channel s maximum delay τ_s (normalized to the system's sampling interval Δt) is short enough so that the adjacent CIR replicas in (19) to not overlap (fulfils the sampling theorem),

$$\tau_s \le \frac{N_C}{N_f n_S}, \tag{20}$$

(19) can be further simplified to

$$\begin{aligned}\tilde{g}^p[n] &= \theta_{\mathrm{ini}}N_C^{1/2}N_f^{-1}\exp\left[j(w_o-\hat{w})n\right] \times \sum_{s=0}^{n_S-1}\exp\left[-j\frac{2\pi}{Nc}k_{\mathrm{ini}}\left(n-\frac{s}{n_S}N_t\right)\right]\tilde{h}_s\left[n-\frac{s}{n_S}N_t\right] \\ &\quad \times \sum_{m=0}^{N_f-1}\exp\left[j(w_o-\hat{w})mN_t\right],\end{aligned} \tag{21}$$

that clearly shows that the pilot-dependent samples are limited to the n_S sets of samples $\{L_p\}$ (with L_p elements), where the corresponding phase-shifted CIRs have energy. The remaining samples will depend only on the transmitted data and noise.

The elements of $\tilde{\mathbf{g}}^d$ can be expressed by

$$\begin{aligned}\tilde{g}^d[n] &= \sum_{m=0}^{N_f-1}\exp\left(-j2\pi k_{\mathrm{ini}}\frac{n+mN_t}{N_C}\right) \times \exp\left[-j\hat{w}(n+mN_t)\right]\tilde{r}^d[n+mN_t] \\ &= \theta_{\mathrm{ini}}N_C^{-1/2} \times \sum_{m=0}^{N_f-1}\left(\exp\left(-j2\pi k_{\mathrm{ini}}\frac{n+mN_t}{N_C}\right) \times \exp\left[j(w_o-\hat{w})(n+mN_t)\right] \times \sum_{s=0}^{n_S-1}\sum_{l=0}^{L-1}\sum_{\substack{k=0\\k\notin\wp}}^{N_C-1}\tilde{h}_s[l]d_s[k] \times \exp\left[j\frac{2\pi}{N_C}k(n-l+mN_t)\right]\right) \\ &= \theta_{\mathrm{ini}}N_C^{-1/2}\exp\left[j(w_o-\hat{w})n\right]\exp\left(-j2\pi k_{\mathrm{ini}}\frac{n}{N_C}\right) \times \sum_{s=0}^{n_S-1}\sum_{l=0}^{L-1}\tilde{h}_s[l]\Psi,\end{aligned} \tag{22}$$

where

$$\begin{aligned}\Psi &= \sum_{\substack{k=0\\k\notin\wp}}^{N_C-1}d_s[k]\exp\left[j\frac{2\pi}{N_C}k(n-l)\right] \times \sum_{m=0}^{N_f-1}\exp\left[j(w_o-\hat{w})mN_t\right]\exp\left[j\frac{2\pi}{N_f}(k-k_{\mathrm{ini}})m\right] \\ &= \sum_{\substack{k=0\\k\notin\wp}}^{N_C-1}d_s[k]\exp\left[j\frac{2\pi}{N_C}k(n-l)\right] \times \sum_{m=0}^{N_f-1}\exp\left[j\frac{2\pi m}{N_f}\left[(f_o-\hat{f})N_C\Delta t+(k-k_{\mathrm{ini}})\right]\right],\end{aligned} \tag{23}$$

where $\hat{f}$ is the initial candidate frequency offset.

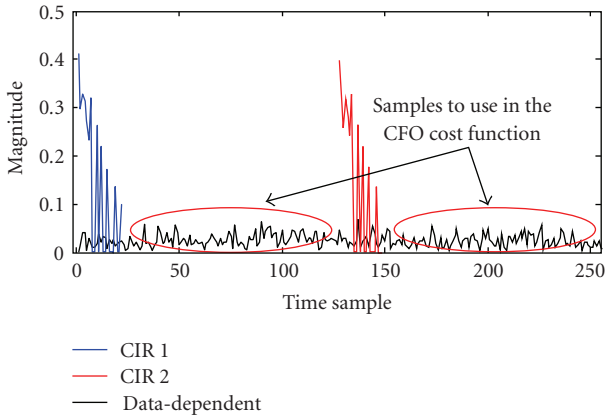

Figure 2: Example of the constitution of vector $\tilde{\mathbf{g}}$.

The elements of the noise vector $\tilde{\mathbf{v}}$ can be expressed by

$$\tilde{v}[n] = \sum_{m=0}^{N_f-1} \exp\left(-j2\pi k_{\text{ini}} \frac{n+mN_t}{N_C}\right) \times \exp\left[-j\hat{w}(n+mN_t)\right]\tilde{n}[n+mN_t]. \tag{24}$$

Figure 2 depicts an example of the constitution of vector $\tilde{\mathbf{g}}$ for a system with 2 transmission antennas, $N_C = 1024$ subcarriers and pilot separation $N_f = 4(N_t = 256)$. The plots put in evidence that the CIRs energy is limited to 2 sets of samples and the data-dependent component spans the entire symbol duration.

A careful inspection of (23) reveals that the factor Ψ (and the data-dependent component) is zero for

$$\{\phi = (f_o - \hat{f})N_C\Delta t + (k - k_{\text{ini}}) : \phi \in \mathbb{Z} \wedge \phi \neq mN_f,\ m \in \mathbb{Z}\}, \tag{25}$$

independently of the considered sample. Keeping in mind that $k \notin \wp$ and $(k - k_{\text{ini}}) \neq mN_f$, $m \in \mathbb{Z}$, the solution for (25) is

$$(f_o - \hat{f})N_C\Delta t = mN_f \Longleftrightarrow (f_o - \hat{f}) = \frac{mN_f}{N_C\Delta t} = mN_f\Delta f, \quad m \in \mathbb{Z}, \tag{26}$$

where Δf is the subcarrier separation. It should be noted that the solution in (26) presents a periodicity $N_f\Delta f$ and includes the condition when the CFO is completely eliminated ($f_o - \hat{f} = 0$). A similar analysis reveals that the factor Ψ has maximum magnitude for

$$\{\gamma = (f_o - \hat{f})N_C\Delta t : \gamma \in \mathbb{Z} \wedge \gamma \neq mN_f,\ m \in \mathbb{Z}\} \Longrightarrow (f_o - \hat{f}) = \frac{l}{N_C\Delta t} = l\Delta f, \quad l \in \mathbb{Z} \wedge l \neq mN_f. \tag{27}$$

We can conclude that Ψ has minimum values spread $N_f\Delta f$ Hz, with $(N_f - 1)$ maximum magnitude values in between, separated by Δf Hz.

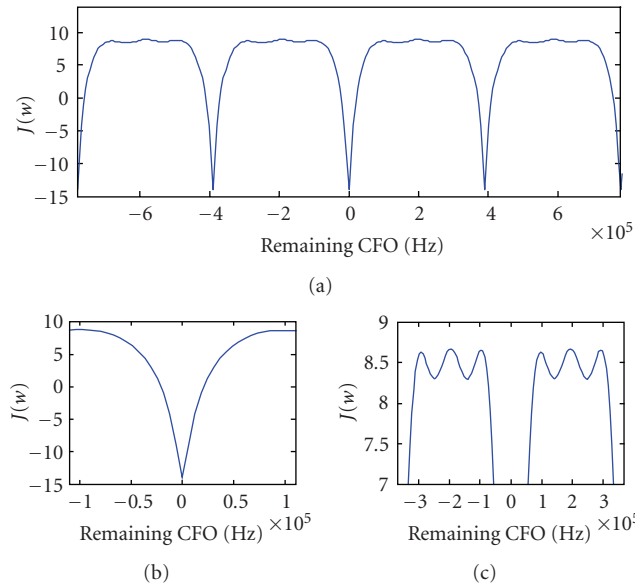

Figure 3: The cost function $J(w)$.

Let us define the column $(N_t - n_S L_p)$-vector $\mathbf{j}$ that collects the samples of $\tilde{\mathbf{g}}$ with no CIRs energy (only data-dependent and noise; example depicted in Figure 2) and the cost function $J(\hat{w})$ as the energy in $\mathbf{j}$:

$$J(\hat{w}) = \mathbf{j}^H\mathbf{j}. \tag{28}$$

The definition of the cost function guarantees that, if within the acquisition range, its minimum value will converge to the true estimate as the number of elements in $\mathbf{j}$ increases (and the noise term tends to a floor in $J(\hat{w})$). The elements in $\mathbf{j}$ may be obtained from one OFDM symbol or a set of symbols (with data and pilots) if higher accuracy on the estimate is required. From the previous analysis of the factor Ψ, it is clear that the acquisition range of our cost function is $]-N_f\Delta f/2, N_f\Delta f/2[$. The CFO estimate can be found by a line search within the acquisition range to find the minimum value of the cost function:

$$\hat{w}_o = \arg\left\{\min_{\hat{w}} J(\hat{w})\right\}, \tag{29}$$

where $\hat{w}_o$ is the estimated CFO value. The exhaustive line search is computationally demanding, depending on the search's granularity. Hence, there is a tradeoff between complexity and estimate's variance.

The cost function has a closed form expression, and its behavior is perfectly described. In the acquisition range, there are N_f maximum values; in the interval limited by the maximum values that surround the perfect estimate, $J(\hat{w})$ presents a smooth shape with a single minimum. Using the knowledge we possess of the cost function, we propose a 2-step approach to find its minimum value. The initial step performs a coarse line search to locate the global minimum interval. Testing N_f candidate CFO values evenly spaced by Δf Hz should suffice. The candidate CFO will be the one with the lowest cost. If the number of elements in

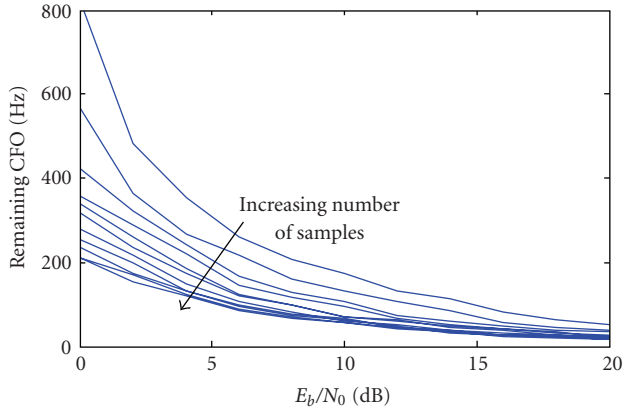

FIGURE 4: Estimated CFO standard deviation versus the number of samples in $J(w)$.

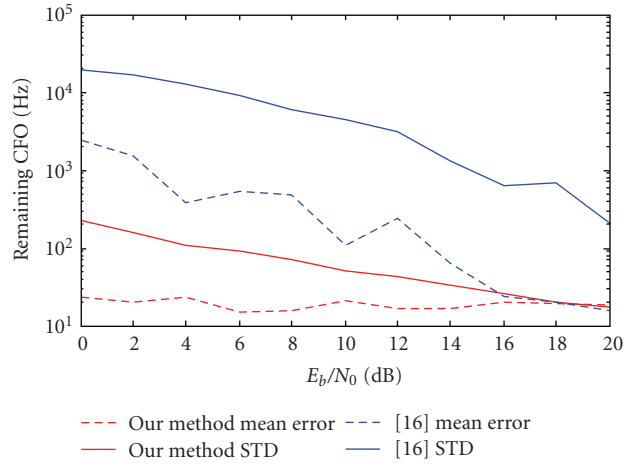

FIGURE 5: Remaining CFO.

j is small and *SNR* is very low, the probability of wrong identification may not be negligible and the number of candidate CFO values can be increased thus decreasing the wrong identification probability. In the final step, we use the gradient descent method [26] to find the global minimum.

Figure 3 depicts an example of the cost function for a 2×1 Alamouti OFDM system with $N_C = 1024$ subcarriers, sampling interval $\Delta t = 10$ nanoseconds and pilot separation $N_f = 4$. The values in the plot were acquired using an $SNR = 20$ dB. In Figure 3(a), the separation of ≈390 kHz between consecutives minimum values is visible. Figure 3(b) shows in detail the interval around $(w_o - \hat{w}) = 0$. It is clear that it has a unique global minimum that is easy to find (no problem with local minimum values). In Figure 3(c), the $N_f - 1$ maximum values between consecutive minimum values are clearly visible. It also shows in detail that the separation of the maximum values around $(w_o - \hat{w}) = 0$ is ≈195 kHz.

Figure 4 shows the evolution of the estimated CFO standard deviation with the number of samples used in estimation algorithm (elements of **j**). The plots depict the standard deviation when the number of samples goes from 200 to 2000, in steps of 200 samples.

3.3. Channel Estimation. Assuming that the CFO is completely eliminated, the output of the initial operation of the CFO algorithm is made up of the pilot-dependent component and noise $\tilde{\mathbf{g}} = \tilde{\mathbf{g}}^p + \tilde{\mathbf{v}}$. The data-dependent component was eliminated from this vector, opening way to easily obtain an initial CIR estimate.

The channel estimation algorithm starts by isolating each of the n_S phase-shifted CIRs from $\tilde{\mathbf{g}}$ and removing the modulating exponential factor. The elements of the resulting vectors $\hat{\tilde{\mathbf{h}}}_{s,LS}$ can be expressed by

$$\begin{aligned}\hat{\tilde{h}}_{s,LS}[n] &= \exp\left[j\frac{2\pi}{Nc}k_i n\right]\sum_{m=0}^{N_t-1}\delta\left[n+\frac{s}{n_S}N_t-m\right]\tilde{g}[n]\\ &= \theta_i N_C^{1/2}N_f^{-1}\tilde{h}_s[n]+\exp\left[j\frac{2\pi}{Nc}k_i n\right]\tilde{v}_i\left[n+\frac{s}{n_S}N_t\right].\end{aligned} \tag{30}$$

In [24], it was demonstrated that for a single transmitting antenna OFDM system with perfect synchronization, (30) is the TD counterpart of FD LS estimate. By using phase-shifted pilot sequences that allow the separation of the different CIRs, the same result holds in the present model.

This initial estimate can be significantly improved by incorporating a TD linear minimum MSE (LMMSE) filter $\mathbf{W}_s$ to reduce the estimate's error, taking advantage of the CIR energy concentration. The improvements provided by this filter are especially significant for low values of SNR.

The LMMSE filter can be expressed by [27]

$$\mathbf{W}_s = \operatorname{diag}\left(\frac{\sigma^2_{h_s}[0]}{\sigma^2_{h_s}[0]+N_t^{-1}\sigma^2_{\mathbf{n}}},\ldots,\frac{\sigma^2_{h_s}[L_p-1]}{\sigma^2_{h_s}[L_p-1]+N_t^{-1}\sigma^2_{\mathbf{n}}},0,\ldots,0\right). \tag{31}$$

The resulting CIR and CFR estimates are, respectively, $\hat{\tilde{\mathbf{h}}}_s = \mathbf{W}_s\hat{\tilde{\mathbf{h}}}_{s,LS}$ and $\hat{\mathbf{h}}_s = \mathbf{F}\hat{\tilde{\mathbf{h}}}_s$.

4. Simulation Results

A simulation scenario was implemented using an Alamouti 2×1 OFDM system with $Nc = 1024$ modulated subcarriers, sampling interval $\Delta t = 50$ nanoseconds and a CP with 100 samples. The transmitted OFDM symbols carried pilots and data, with a pilot separation $Nf = 8$. The OFDM frame consists of 16 symbols. The CFO value was randomly generated in each frame with a value inside the acquisition range $]-N_f\Delta f/2, N_f\Delta f/2[$. The CFO estimation and removal was performed on a frame basis. Two channel models with exponentially decaying power delay profile (PDP) were used to simulate indoor (50 nanoseconds *rms* delay spread) and outdoor environments (250 nanoseconds *rms* delay spread). To validate the proposed method, several simulations were performed using Eb/N0 values in the range of 0 dB to 20 dB.

Figure 5 shows the remaining CFO at the output of the CFO mitigate block when using the indoor channel model. The dashed lines represent the average remaining

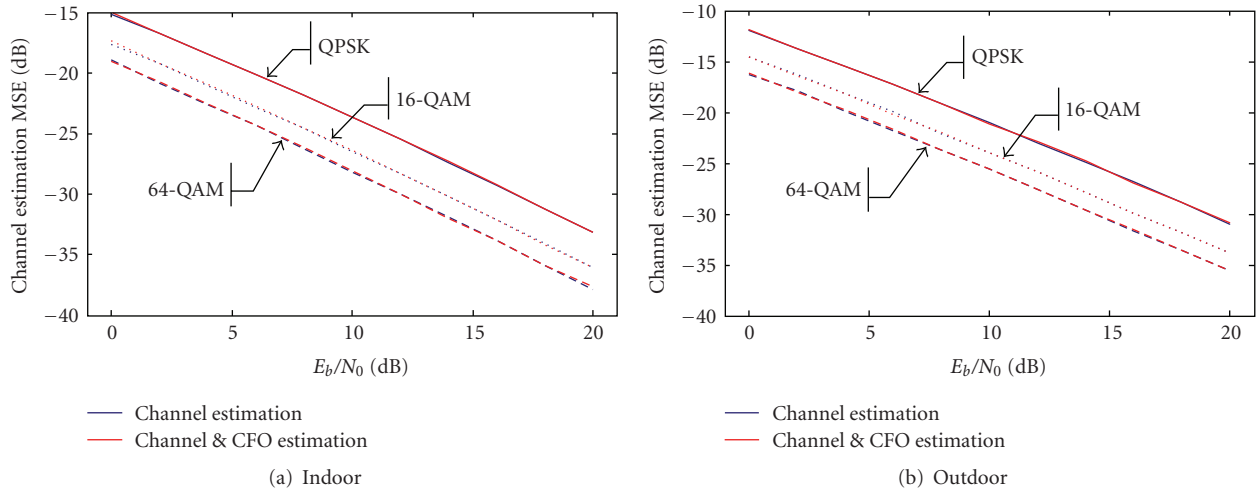

Figure 6: Joint channel and CFO estimation MSE.

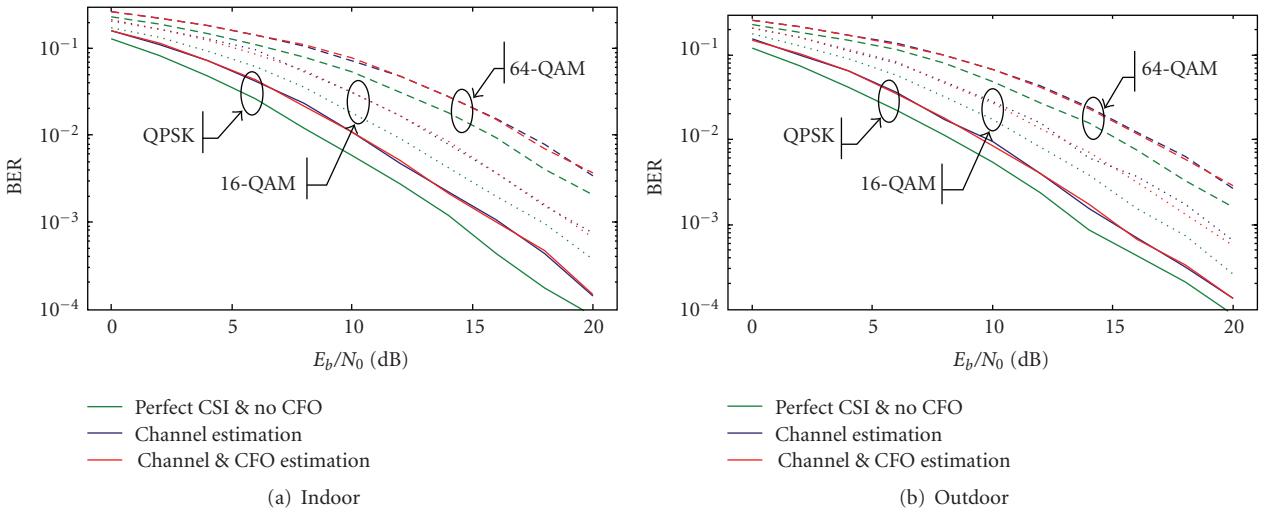

Figure 7: System BER performance.

CFO. The solid lines represent the standard deviation of the CFO estimate. In our method, the gradient descent was stopped for a step of 10 HZ. For the method in [16], one null subcarrier was added to each OFDM symbol, and an exhaustive search was performed with a 10 HZ step. The results show that our method is unbiased for the all range of Eb/N0 values. The algorithm generates estimates with small deviation from the true value using a limited number of symbols (16). The estimate deviation is ~1% of that of [16] for low values of *SNR*. The method in [16] requires a large number of symbols and/or more receive antennas to generate accurate estimates. This result shows that the investigated method is quite adequate for burst systems.

Figure 6 depicts the MSE of the channel estimation algorithm (blue plots) when the system has perfect synchronization and the MSE of the joint CFO and channel estimation process (red plots), when using QPSK, 16-QAM, and 64-QAM modulations. Figure 6(a) presents the results for the indoor channel and Figure 6(b) for the outdoor channel.

Figure 7 depicts the system BER for 3 scenarios: the ideal situation where the receiver has perfect channel state information (CSI) (with no pilot overhead) and the CFO is absent (green plots), the situation when the receiver must estimate the channel from the received samples (blue plots), and the more realistic scenario where the receiver needs to estimate both the CFO and channel (red plots). Simulations results were obtained also for QPSK, 16-QAM, and 64-QAM modulations as identified in the figures. Figure 7(a) presents the results for the indoor channel and Figure 7(b) for the outdoor channel.

The channel estimation MSE improvement that can be observed for higher-order modulations is due to the fact that the ratio between the powers in the pilot symbols and data symbols is kept constant in all simulations. The large increase of delay spread between both channels is the origin of the ~3 dB MSE degradation when moving from the

indoor channel to the outdoor channel plots. This acceptable degradation shows the ability of the estimator to deal with the increasing channel delay spread by always weighing the energy of channel taps versus noise variance. The channel estimation BER plots present a degradation of ~1,2 dB that can be largely attributed to the 12.5% pilot overhead.

The joint CFO and channel estimation MSE is an effective measure of the degradation caused by both algorithms. In these plots, the estimated channel was compared against the true channel affected by the same CFO that distorted the received signal (according to (10)). The results plotted in Figures 6 and 7 show that the performance degradation of the joint process is marginal when compared with channel estimation only, substantiating the performance of the proposed algorithms.

5. Conclusions

We have investigated a CFO estimation algorithm and an associated channel estimation block for OFDM with transmitter diversity that explores the TD structure of transmitted symbols carrying pilots and data. The CFO algorithm relies solely on the data component present on the symbols to estimate the CFO, avoiding additional overhead like training symbols or null subcarriers. Simulation results show that the residual CFO has a minimal impact in the system's performance, confirming that the CFO estimates have minimal deviation from the true value. The definition and shape of the cost function determine a very low-complexity scheme. An intermediate output of the CFO algorithm provides an easy to get initial CIR estimate minimizing the overall complexity. By incorporating a TD LMMSE filter, the initial CIR estimate is significantly improved. Simulation results of the joint algorithms confirm a reduced degradation of the system's performance when compared with the ideal scenario.

Acknowledgments

The authors wish to thank Fundação para a Ciência e a Tecnologia that partially supported this work through the project "PHOTON—Distributed and Extendible Heterogeneous Radio Architectures using Fibre Optic Networks" (PTDC/EEA-TEL/72890/2006).

References

[1] R. van Nee and R. Prasad, *OFDM for Wireless Multimedia Communications*, Artech House, London, UK, 1st edition, 2000.

[2] G. L. Stüber, J. R. Barry, S. W. McLaughlin, Y. Li, M. A. Ingram, and T. G. Pratt, "Broadband MIMO-OFDM wireless communications," *Proceedings of the IEEE*, vol. 92, no. 2, pp. 271–294, 2004.

[3] H. Sampath, S. Talwar, J. Tellado, V. Erceg, and A. Paulraj, "A fourth-generation MIMO-OFDM broadband wireless system: design, performance, and field trial results," *IEEE Communications Magazine*, vol. 40, no. 9, pp. 143–149, 2002.

[4] A. J. Paulraj, D. A. Gore, R. U. Nabar, and H. Bölcskei, "An overview of MIMO communications—a key to gigabit wireless," *Proceedings of the IEEE*, vol. 92, no. 2, pp. 198–218, 2004.

[5] IEEE Std 802.11, "Wireless LAN medium access control (MAC) and physical layer (PHY) specifications: high-speed physical layer in the 5 GHz band," 1999.

[6] I. Koffman and V. Roman, "Broadband wireless access solutions based on OFDM access in IEEE 802.16," *IEEE Communications Magazine*, vol. 40, no. 4, pp. 96–103, 2002.

[7] K. Sathananthan and C. Tellambura, "Probability of error calculation of OFDM systems with frequency offset," *IEEE Transactions on Communications*, vol. 49, no. 11, pp. 1884–1888, 2001.

[8] T. Pollet, M. Van Bladel, and M. Moeneclaey, "BER sensitivity of OFDM systems to carrier frequency offset and Wiener phase noise," *IEEE Transactions on Communications*, vol. 43, no. 2–4, pp. 191–193, 1995.

[9] L. Rugini and P. Banelli, "BER of OFDM systems impaired by carrier frequency offset in multipath fading channels," *IEEE Transactions on Wireless Communications*, vol. 4, no. 5, pp. 2279–2288, 2005.

[10] J.-J. van de Beek, M. Sandell, and P. O. Börjesson, "ML estimation of time and frequency offset in OFDM systems," *IEEE Transactions on Signal Processing*, vol. 45, no. 7, pp. 1800–1805, 1997.

[11] H. Bölcskei, "Blind high-resolution uplink synchronization of OFDM-based multiple access schemes," in *Proceedings of the 2nd IEEE Workshop on Signal Processing Advances in Wireless Communications (SPAWC '99)*, pp. 166–169, Annapolis, Md, USA, May 1999.

[12] N. Lashkarian and S. Kiaei, "Class of cyclic-based estimators for frequency-offset estimation of OFDM systems," *IEEE Transactions on Communications*, vol. 48, no. 12, pp. 2139–2149, 2000.

[13] T. M. Schmidl and D. C. Cox, "Robust frequency and timing synchronization for OFDM," *IEEE Transactions on Communications*, vol. 45, no. 12, pp. 1613–1621, 1997.

[14] M. Morelli and U. Mengali, "Improved frequency offset estimator for OFDM applications," *IEEE Communications Letters*, vol. 3, no. 3, pp. 75–77, 1999.

[15] H. Liu and U. Tureli, "A high-efficiency carrier estimator for OFDM communications," *IEEE Communications Letters*, vol. 2, no. 4, pp. 104–106, 1998.

[16] X. Ma, M.-K. Oh, G. B. Giannakis, and D.-J. Park, "Hopping pilots for estimation of frequency-offset and multiantenna channels in MIMO-OFDM," *IEEE Transactions on Communications*, vol. 53, no. 1, pp. 162–172, 2005.

[17] Y. Li, N. Seshadri, and S. Ariyavisitakul, "Channel estimation for OFDM systems with transmitter diversity in mobile wireless channels," *IEEE Journal on Selected Areas in Communications*, vol. 17, no. 3, pp. 461–471, 1999.

[18] Y. Li, "Simplified channel estimation for OFDM systems with multiple transmit antennas," *IEEE Transactions on Wireless Communications*, vol. 1, no. 1, pp. 67–75, 2002.

[19] M. Shin, H. Lee, and C. Lee, "Enhanced channel-estimation technique for MIMO-OFDM systems," *IEEE Transactions on Vehicular Technology*, vol. 53, no. 1, pp. 261–265, 2004.

[20] H. Zhang, Y. Li, A. Reid, and J. Terry, "Channel estimation for MIMO OFDM in correlated fading channels," in *Proceedings of IEEE International Conference on Communications (ICC '05)*, vol. 4, pp. 2626–2630, Seoul, Korea, May 2005.

[21] H. Zamiri-Jafarian and S. Pasupathy, "Robust and improved channel estimation algorithm for MIMO-OFDM systems,"

IEEE Transactions on Wireless Communications, vol. 6, no. 6, pp. 2106–2113, 2007.

[22] I. Barhumi, G. Leus, and M. Moonen, "Optimal training design for MIMO OFDM systems in mobile wireless channels," *IEEE Transactions on Signal Processing*, vol. 51, no. 6, pp. 1615–1624, 2003.

[23] H. Minn and N. Al-Dhahir, "Optimal training signals for MIMO OFDM channel estimation," in *Proceedings of IEEE Global Telecommunications Conference (GLOBECOM '04)*, vol. 1, pp. 219–224, Dallas, Tex, USA, November-December 2004.

[24] C. Ribeiro and A. Gameiro, "Direct time-domain channel impulse response estimation for OFDM-based systems," in *Proceedings of the 66th IEEE Vehicular Technology Conference (VTC '07)*, pp. 1082–1086, Baltimore, Md, USA, September-October 2007.

[25] M. Morelli, A. N. D'Andrea, and U. Mengali, "Frequency ambiguity resolution in OFDM systems," *IEEE Communications Letters*, vol. 4, no. 4, pp. 134–136, 2000.

[26] S. Boyd and L. Vandenberghe, *Convex Optimization*, Cambridge University Press, Cambridge, UK, 2004.

[27] J.-J. van de Beek, O. Edfors, M. Sandell, S. K. Wilson, and P. O. Börjesson, "On channel estimation in OFDM systems," in *Proceedings of the 45th IEEE Vehicular Technology Conference (VTC '95)*, vol. 2, pp. 815–819, Chicago, Ill, USA, July 1995.